Modulation of Coordination Chemistry in Copper(I) Complexes Supported by Bis[2-(2-pyridyl)ethyl]amine-Based Tridentate Ligands

Takao Osako,[†] Yoshimitsu Tachi,[†] Masayasu Taki,[‡] Shunichi Fukuzumi,*[,‡] and Shinobu Itoh*[,†]

Department of Chemistry, Graduate School of Science, Osaka City University, 3−3−138, Sugimoto, Sumiyoshi-ku, Osaka, 558-8585, Japan, and Department of Material and Life Science, Graduate School of Engineering, Osaka University, CREST, Japan Science and Technology Corporation, 2−1 Yamada-oka, Suita, Osaka 565-0871, Japan

Received June 12, 2001

Structure and physicochemical properties of copper(I) complexes of the tridentate ligands $\mathbf{L^2}$ (*N*,*N*-bis[2-(6-methylpyridin-2-yl)ethyl]phenethylamine) and $\mathbf{L^3}$ (*N*,*N*-bis[2-(2-pyridyl)ethyl]-*β*-methylphenethylamine) have been examined to obtain deeper insights into modulation of the coordination chemistry of copper(I) complexes. $[Cu^I(\mathbf{L^2})(CH_3CN)](ClO_4)$ (**2**·CH_3CN) has a distorted tetrahedral geometry, which consists of three nitrogen atoms of the ligand and one nitrogen atom of the bound CH_3CN. Steric repulsion between the 6-methyl group on the pyridine nucleus of $\mathbf{L^2}$ and the metal ion of the complex prevents the cuprous complex from adaptation to a three-coordinate geometry which must have a shorter Cu−N(pyridine) distance (∼1.88 Å). Thus, the four-coordinate copper(I) complex (**2**·CH_3CN) with a longer Cu−N bond (1.98∼2.13 Å) becomes favorable, resulting in rather strong binding of CH_3CN to the metal ion. In $[Cu^I(\mathbf{L^3})](ClO_4)$ (**3**), there is a $Cu^I-\pi$ interaction between the cuprous ion and the phenyl group of the ligand sidearm. Such a copper(I)−arene interaction is essentially weak, but is significantly stabilized in complex **3**. The methyl group at the benzylic position of $\mathbf{L^3}$ reduces the degree of freedom of sidearm rotation to make the phenyl group stick on the cuprous ion. Thus, the reactivity of the copper(I) complexes of $\mathbf{L^2}$ and $\mathbf{L^3}$ toward dioxygen is significantly diminished, showing sharp contrast to the high reactivity of the copper(I) complex supported by a similar tridentate ligand $\mathbf{L^1}$ (*N*,*N*-bis[2-(2-pyridiyl)ethyl]-phenethylamine).

Introduction

Great success has been brought about in copper/dioxygen chemistry using a variety of bis[2-(2-pyridyl)ethyl]amine-based tridentate ligands.[1] Karlin and co-workers first developed a series of dinuclear copper(I) complexes supported by dinucleating ligands containing two bis[2-(2-pyridyl)ethyl]amine units, and they succeeded in mimicking the structures and functions of the active sites of hemocyanin and tyrosinase (reversible O_2 binding and aromatic ligand hydroxylation).[2] Such pioneering works by Karlin and co-workers attracted many researchers in the related area to open the new field of copper/dioxygen bioinorganic chemistry.[1,3] Our contribution in this field is finding quantitative aliphatic ligand hydroxylation with a mononuclear copper complex of ligand $\mathbf{L^1}$ (*N*,*N*-bis[2-(2-pyridiyl)ethyl]-phenethylamine, Chart 1).[4] Namely, a (μ-η^2:η^2-peroxo)dicopper(II) complex (**A** in Scheme 1), generated by treating $[Cu^I(\mathbf{L^1})]^+$ with O_2 or $[Cu^{II}(\mathbf{L^1})]^{2+}$ with H_2O_2 at a low temperature (−80 °C), decomposes, leading to benzylic hydroxylation of its ligand sidearm to give $\mathbf{L^{1-OH}}$ (Chart 1). Mechanistic studies have suggested that a bis(μ-oxo)dicopper(III) intermediate (**B** in Scheme 1), formed from the peroxo complex (**A**) by O−O bond homolysis, is the actual active oxygen species for the aliphatic C−H bond activation.[5] Réglier et al recently investigated a closely related system.[6]

The structure and reactivity of copper complexes has been demonstrated to alter significantly by introducing a small change in the supporting ligands. One of the most remarkable examples is found in copper/dioxygen chemistry with the TMPA [tris(2-pyridylmethyl)amine] ligand system (Chart 1). The copper(I) complex of TMPA itself afforded a (μ-1,2-peroxo)dicopper(II)

* To whom correspondence should be addressed.
[†] Osaka City University.
[‡] Osaka University.

(1) (a) Kopf, M.-A.; Karlin, K. D. In *Biomimetic Oxidations Catalyzed by Transition Metal Complexes*; Meunier, B., Ed.; Imperial College Press: London, 2000; pp 309−362. (b) Karlin, K. D.; Zuberbühler, A. D. In *Bioinorganic Catalysis*, 2nd ed.; Reedijk, J., Bouwman, E., Eds.; Marcel Dekker: New York, 1999; pp 469−534. (c) Karlin, K. D.; Kaderli, S.; Zuberbühler, A. D. *Acc. Chem. Res*. **1997**, *30*, 139−147. (d) Fox, S.; Karlin, K. D. In *Reactive Oxygen in Biochemistry*; Valentine, J. S., Foote, C. S., Greenberg, A., Liebman, J. F., Eds.; Chapman & Hall: Glasgow, 1995; pp 188−231. (e) Schindler, S. *Eur. J. Inorg. Chem*. **2000**, 2311−2326.

(2) (a) Karlin, K. D.; Haka, M. S.; Cruse, R. W.; Gultneh, Y. *J. Am. Chem. Soc*. **1985**, *107*, 5828−5829. (b) Karlin, K. D.; Gultneh, Y.; Hutchinson, J. P.; Zubieta, J. *J. Am. Chem. Soc*. **1982**, *104*, 5240−5242.

(3) (a) Kitajima, N.; Moro-oka, Y. *Chem. Rev*. **1994**, *94*, 737−757. (b) Tolman, W. B. *Acc. Chem. Res*. **1997**, *30*, 227−237. (c) Blackman, A. G.; Tolman, W. B. In *Metal-Oxo and Metal-Peroxo Species in Catalytic Oxidations*; Meunier, Ed.; Springer: Berlin, 2000; pp 179−211. (d) Mahadevan, V.; Gebbink, R. K.; Stack, T. D. P. *Curr. Opin. Chem. Biol*. **2000**, *4*, 228−234.

(4) Itoh, S.; Kondo, T.; Komatsu, M.; Ohshiro, Y.; Li, C.; Kanehisa, N.; Kai, Y.; Fukuzumi, S. *J. Am. Chem. Soc*. **1995**, *117*, 4714−4715.

(5) (a) Itoh, S.; Nakao, H.; Berreau, L. M.; Kondo, T.; Komatsu, M.; Fukuzumi, S. *J. Am. Chem. Soc*. **1998**, *120*, 2890−2899. (b) Itoh, S.; Taki, M.; Nakao, H.; Holland, P. L.; Tolman, W. B.; Que, L., Jr.; Fukuzumi, S. *Angew. Chem., Int. Ed*. **2000**, *39*, 398−400.

(6) (a) Blain, I.; Bruno, P.; Giorgi, M.; Lojou, E.; Lexa, D.; Réglier, M. *Eur. J. Inorg. Chem*. **1998**, 1297−1304. (b) Blain, I.; Giorgi, M.; De Riggi, I.; Réglier, M. *Eur. J. Inorg. Chem*. **2000**, 393−398. (c) Blain, I.; Giorgi, M.; De Riggi, I.; Réglier, M. *Eur. J. Inorg. Chem*. **2001**, 205−211.

10.1021/ic010625d CCC: $20.00
Published on Web 11/13/2001

Chart 1

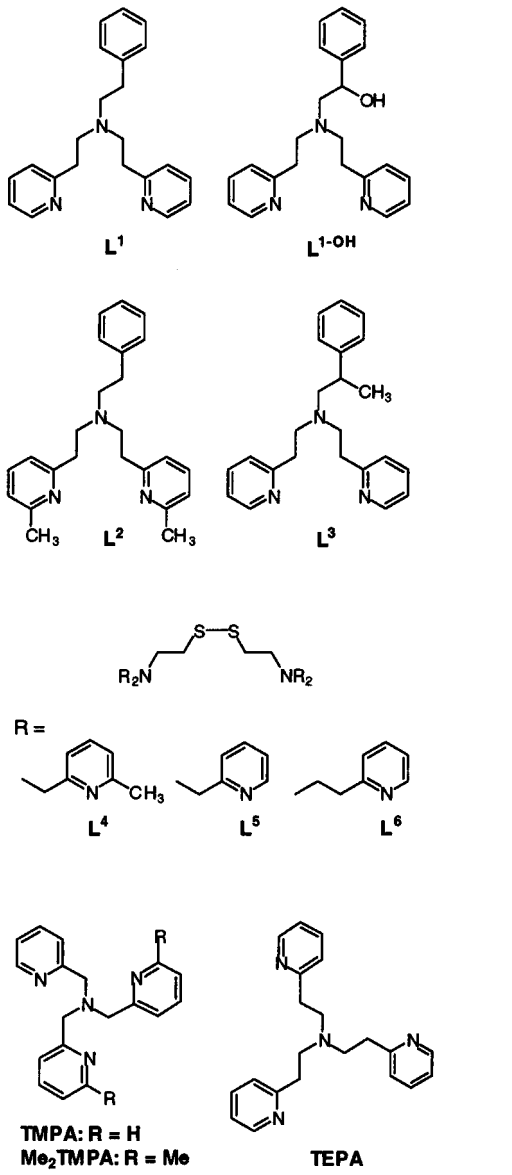

Scheme 1

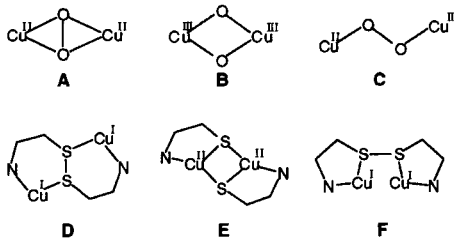

complex (**C** in Scheme 1) in the reaction with O_2 at a low temperature,[7] while introduction of 6-methyl group into two of the three pyridine nuclei of the ligand (Me_2TMPA:bis(6-methyl-2-pyridylmethyl)(2-pyridylmethyl)amine, Chart 1) resulted in formation of a bis(μ-oxo)dicopper(III) complex (**B**) under similar experimental conditions.[8] In this case, a small perturbation in the ligand triggers a drastic change in the oxidation state of metal (Cu^{II} versus Cu^{III}) and oxygen (peroxo versus oxo). Such a drastic change in the structure of copper complexes induced by the 6-methyl substituent has also been found in a copper(I)/disulfide system, where ligand $\mathbf{L^4}$ (Chart 1) affords a disulfide−dicopper(I) complex (type **D** in Scheme 1), and reductive cleavage of the S−S bond of the ligand occurs to give a bis(μ-thiolato)dicopper(II) complex (type **E** in Scheme 1) in the case of ligand $\mathbf{L^5}$ (Chart 1).[9] Such prominent effects of the 6-methyl substituent of the pyridyl ligands have also been observed in the related iron chemistry.[10]

Effects of the alkyl linker chain in the tetradentate ligand system (methylene in TMPA versus ethylene in TEPA, tris(2-pyridylethyl)amine, Chart 1) have also been investigated to demonstrate that the longer ethylene linker of TEPA can adapt its cuprous complex to a tetrahedral geometry, stabilizing the Cu(I) state of the complex.[11] Thus, the copper(I) complex of TEPA does not react with O_2; this is in sharp contrast to the high reactivity of the copper(I) complex of TMPA.[7] In the copper(I)/disulfide case as well, ligand $\mathbf{L^6}$ (Chart 1) with the ethylene linker between the tertiary amine nitrogen and the pyridine nucleus affords a different type of disulfide−dicopper-(I) complex (type **F** in Scheme 1).[9]

In our continuing effort to clarify the ligand effects on the copper/dioxygen reactivity, we report herein the substituent effects on the structure and reactivity of copper(I) complexes supported by bis[2-(2-pyridyl)ethyl]amine-based tridentate ligands, $\mathbf{L^2}$ and $\mathbf{L^3}$ (Chart 1). Only one methyl substitution either at the 6-position of the pyridine nucleus or at the benzylic position of the ligand sidearm of $\mathbf{L^1}$ resulted in a drastic change in the structure and reactivity of the copper(I) complexes, providing further insight into the ligand control of copper/dioxygen chemistry.

Results and Discussion

Synthesis of Ligands and Copper(I) Complexes. Ligands $\mathbf{L^2}$ and $\mathbf{L^3}$ were prepared by a Michael addition of phenethylamine to 6-methyl-2-vinylpyridine and of β-methylphenethylamine to 2-vinylpyridine, respectively, in refluxing methanol under acidic conditions. The copper(I) complexes of $\mathbf{L^2}$ and $\mathbf{L^3}$ were obtained by treating the ligand with an equimolar amount of $[Cu^I(CH_3CN)_4](ClO_4)$ in CH_2Cl_2 under anaerobic conditions (in a glovebox). All compounds gave satisfactory results in the elemental and MS analyses (see Experimental).

Crystal Structure. Crystal structures of the copper(I) complexes of ligands $\mathbf{L^2}$ and $\mathbf{L^3}$, $[Cu^I(\mathbf{L^2})(CH_3CN)](ClO_4)$ (**2**·CH_3-CN) and $[Cu^I(\mathbf{L^3})](ClO_4)$ (**3**), have been determined by X-ray crystallographic analysis, as shown in Figures 1 and 2. The crystallographic data and selected bond lengths and angles are summarized in Table 1 and Tables 2 and 3, respectively. Despite our great efforts, single crystals of the copper(I) complex of ligand $\mathbf{L^1}$, $[Cu^I(\mathbf{L^1})](ClO_4)$ (**1**),[5a] suitable for X-ray crystallographic analysis have not been obtained so far. Thus, we used

(7) Jacobson, R. R.; Tyeklar, Z.; Farooq, A.; Karlin, K. D.; Liu, S.; Zubieta, J. *J. Am. Chem. Soc.* **1988**, *110*, 3690−3692.
(8) Hayashi, H.; Fujinami, S.; Nagatomo, S.; Ogo, S.; Suzuki, M.; Uehara, A.; Watanabe, Y.; Kitagawa, T. *J. Am. Chem. Soc.* **2000**, *122*, 2124−2125.
(9) Itoh, S.; Nakagawa, M.; Fukuzumi, S. *J. Am. Chem. Soc.* **2001**, *123*, 4087−4088.
(10) (a) Zang, Y.; Elgren, T. E.; Dong, Y.; Que, L., Jr. *J. Am. Chem. Soc.* **1993**, *115*, 811−813. (b) Que, L., Jr.; Dong, Y. *Acc. Chem. Res.* **1996**, *29*, 190−196. (c) Zheng, H.; Zang, Y.; Dong, Y.; Young, V. G., Jr.; Que, L., Jr. *J. Am. Chem. Soc.* **1999**, *121*, 2226−2235. (d) Chen, K.; Que,L., Jr. *Angew. Chem., Int. Ed.* **1999**, *38*, 2227−2229. (e) Costas, M.; Tipton, A. K.; Chen, K.; Jo, D.-H.; Que, L., Jr. *J. Am. Chem. Soc.* **2001**, *123*, 6722−6723.
(11) (a) Karlin, K. D.; Sherman, S. E. *Inorg. Chim. Acta* **1982**, *65*, L39−L40. (b) Schatz, M.; Becker, M.; Thaler, F.; Hampel, F.; Schindler, S.; Jacobson, R. R.; Tyeklár, Z.; Murthy, N. N.; Ghosh, P.; Chen, Q.; Zubieta, J.; Karlin, K. D. *Inorg. Chem.* **2001**, *40*, 2312−2322.

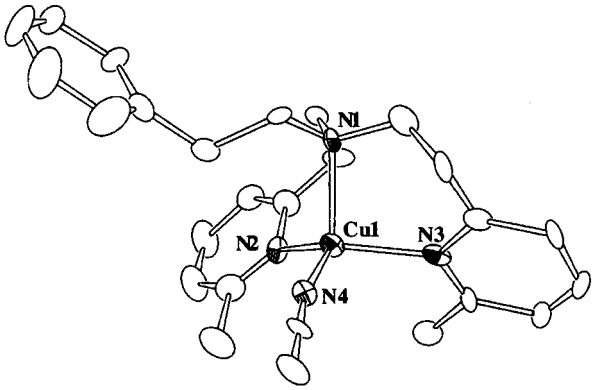

Figure 1. ORTEP drawing of the cationic part of $[Cu^{I}(\mathbf{L^2})(CH_3CN)]ClO_4$ (molecule 1) showing 50% probability thermal ellipsoids. The counteranions and hydrogen atoms are omitted for clarity.

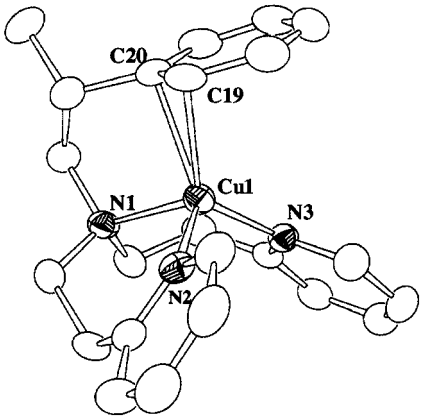

Figure 2. ORTEP drawing of the cationic part of $[Cu^{I}(\mathbf{L^3})]ClO_4$ (molecule 1) showing 50% probability thermal ellipsoids. The counteranions and hydrogen atoms are omitted for clarity.

the reported crystal structures of copper(I) complexes supported by similar tridentate ligands containing the same bis[2-(2-pyridyl)ethyl]amine moiety for comparison.[12,13]

The unit cell of $[Cu^{I}(\mathbf{L^2})(CH_3CN)](ClO_4)$ ($\mathbf{2}\cdot CH_3CN$) consists of two crystallographically independent Cu^{I}-complex ions, including two *N*-bound acetonitrile molecules and two ClO_4^- ions. The cuprous ion in $\mathbf{2}\cdot CH_3CN$ has a distorted tetrahedral geometry with an N4 donor set, one from the bound CH_3CN and the others from the tridentate ligand $\mathbf{L^2}$. Although bond distances and angles between the two molecules (molecule 1 and molecule 2) are different slightly from each other, structural parameters (Cu−N distances and N−Cu−N angles) of $\mathbf{2}\cdot CH_3CN$ are fairly similar to those of the reported dinuclear Cu^{I} complex, $[Cu^{I}_2(N4PY2)(CH_3CN)_2](ClO_4)_2$ ($\mathbf{4}\cdot CH_3CN$), where each copper ion has a pseudotetrahedral geometry supported by the bis[2-(2-pyridyl)ethyl]amine unit and one molecule of CH_3CN (Cu−N distances, 1.945−2.151 Å; N−Cu−N angles, 98.1−122.8°) (Scheme 2).[13] Thus, the 6-methyl group of the pyridine nucleus of $\mathbf{L^2}$ induces little effect on the structure of the four-coordinate copper(I) complex.

On the other hand, Karlin and co-workers have also reported the nearly T-shaped three-coordinate copper(I) complex **5** supported by *N*,*N*-bis[2-(2-pyridyl)ethyl]benzylamine (Scheme 3),[12] where the $Cu-N_{py}$ distances are significantly shorter (1.873, 1.893 Å) than those in $\mathbf{2}\cdot CH_3CN$ and $\mathbf{4}\cdot CH_3CN$. In this study, however, such a three coordinate copper(I) complex could not be obtained when ligand $\mathbf{L^2}$ was employed. This is probably

Table 1. Summary of X-ray Crystallographic Data

	$[Cu^{I}(\mathbf{L^2})(CH_3CN)]ClO_4$	$[Cu^{I}(\mathbf{L^3})]ClO_4$
empirical formula	$C_{26}H_{32}N_4O_4ClCu$	$C_{23}H_{27}N_3O_4ClCu$
formula weight	563.56	508.49
crystal system	triclinic	triclinic
space group	*P*1 (#1)	*P*−1 (#2)
a, Å	11.956(1)	15.621(2)
b, Å	12.073(1)	17.202(2)
c, Å	10.379(1)	8.2593(9)
α, deg	106.494(2)	92.232(6)
β, deg	106.108(5)	90.706(4)
γ, deg	99.266(3)	87.545(4)
V, Å^3	1332.5(2)	2215.6(4)
Z	2	4
F(000)	588.00	1056.00
D_{calc}, g/cm^3	1.405	1.524
T, °C	−115	−100
cryst size, mm	0.30 × 0.30 × 0.20	0.20 × 0.20 × 0.20
μ (Mo Kα), cm^{-1}	9.58	11.42
diffractometer	Rigaku RAXIS−RAPID	Rigaku RAXIS−RAPID
radiation	Mo Kα (0.71069 Å)	Mo Kα (0.71069 Å)
$2\theta_{max}$, deg	55.0	55.0
no. of reflns measd	9468	13360
no. of reflns obsd	4862 [$I > 1.5\sigma(I)$]	6018 [$I > 3.0\sigma(I)$]
no. of variables	714	638
R^a	0.042	0.046
$R_w{}^b$	0.064	0.072

$^a R = \sum||F_o| - |F_c||/\sum|F_o|$. $^b R_w = \{\sum w(|F_o| - |F_c|)^2/\sum wF_o{}^2\}^{1/2}$.

Table 2. Selected Bond Lengths (Å) and Angles (deg) of $[Cu^{I}(\mathbf{L^2})(CH_3CN)]ClO_4$

Molecule 1		Molecule 2	
Cu(1)−N(1)	2.216(7)	Cu(2)−N(5)	2.152(6)
Cu(1)−N(2)	2.054(6)	Cu(2)−N(6)	1.996(7)
Cu(1)−N(3)	2.009(7)	Cu(2)−N(7)	2.133(6)
Cu(1)−N(4)	1.930(8)	Cu(2)−N(8)	2.005(6)
N(1)−Cu(1)−N(2)	98.3(3)	N(5)−Cu(2)−N(6)	98.3(3)
N(1)−Cu(1)−N(3)	96.3(2)	N(5)−Cu(2)−N(7)	96.9(3)
N(2)−Cu(1)−N(3)	122.0(3)	N(6)−Cu(2)−N(7)	123.3(3)
N(1)−Cu(1)−N(4)	113.7(3)	N(5)−Cu(2)−N(8)	114.3(3)
N(2)−Cu(1)−N(4)	122.4(3)	N(6)−Cu(2)−N(8)	124.8(3)
N(3)−Cu(1)−N(4)	101.4(3)	N(7)−Cu(2)−N(8)	96.6(3)

Table 3. Selected Bond Lengths (Å) and Angles (deg) of $[Cu^{I}(\mathbf{L^3})]ClO_4$

Molecule 1		Molecule 2	
Cu(1)−N(1)	2.113(4)	Cu(2)−N(4)	2.113(3)
Cu(1)−N(2)	2.031(4)	Cu(2)−N(5)	2.024(4)
Cu(1)−N(3)	2.003(4)	Cu(2)−N(6)	1.980(4)
Cu(1)−C(19)	2.251(4)	Cu(2)−C(42)	2.242(4)
Cu(1)−C(20)	2.375(5)	Cu(2)−C(43)	2.189(4)
C(15)−C(16)	1.367(8)	C(38)−C(39)	1.370(7)
C(15)−C(20)	1.389(7)	C(38)−C(43)	1.403(6)
C(16)−C(17)	1.383(8)	C(39)−C(40)	1.405(7)
C(17)−C(18)	1.368(8)	C(40)−C(41)	1.366(6)
C(18)−C(19)	1.397(7)	C(41)−C(42)	1.413(6)
C(19)−C(20)	1.382(7)	C(42)−C(43)	1.404(6)
N(1)−Cu(1)−N(2)	102.2(2)	N(4)−Cu(2)−N(5)	100.6(1)
N(1)−Cu(1)−N(3)	100.1(1)	N(4)−Cu(2)−N(6)	100.1(1)
N(2)−Cu(1)−N(3)	113.7(2)	N(5)−Cu(2)−N(6)	111.4(2)
N(1)−Cu(1)−C(19)	111.9(2)	N(4)−Cu(2)−C(42)	98.2(2)
N(2)−Cu(1)−C(19)	97.9(2)	N(5)−Cu(2)−C(42)	139.8(2)
N(3)−Cu(1)−C(19)	129.5(2)	N(6)−Cu(2)−C(42)	99.8(2)
N(1)−Cu(1)−C(20)	82.5(2)	N(4)−Cu(2)−C(43)	87.5(1)
N(2)−Cu(1)−C(20)	124.3(2)	N(5)−Cu(2)−C(43)	108.9(2)
N(3)−Cu(1)−C(20)	120.0(2)	N(6)−Cu(2)−C(43)	136.6(2)
C(19)−Cu(1)−C(20)	34.6(2)	C(42)−Cu(2)−C(43)	36.9(2)

(12) Blackburn, N. J.; Karlin, K. D.; Concannon, M.; Hayes, J. C.; Gultneh, Y.; Zubieta, J. *Chem. Commun.* **1984**, 939−940.
(13) Karlin, K. D.; Haka, M. S.; Cruse, R. W.; Meyer, G. J.; Farooq, A.; Gultneh, Y.; Hayes, J. C.; Zubieta, J. *J. Am. Chem. Soc.* **1988**, *110*, 1196−1207.

Scheme 2

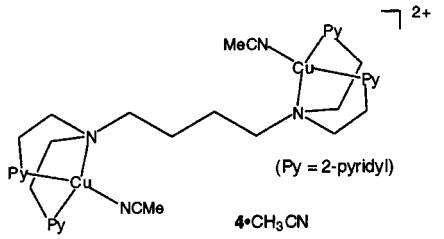

Scheme 3

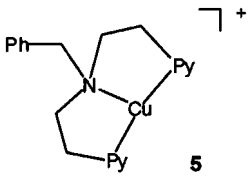

Scheme 4

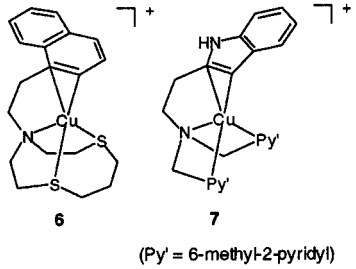

due to the steric effect of the 6-methyl group in $\mathbf{L^2}$, which prohibits formation of such a three-coordinate copper(I) complex having the shorter $Cu-N_{py}$ distance. It has previously been demonstrated that the donor ability of the pyridine nucleus carrying the 6-methyl group is diminished due to the steric repulsion between the methyl group and metal ion.[10a,14] Thus, only the four-coordinate tetrahedral geometry with the longer Cu−N distance is available in the $\mathbf{L^2}$ ligand system. Consequently, removal of the bound CH_3CN from **2**·CH_3CN becomes difficult. This point will be discussed later in more detail.

The copper(I) complex $[Cu^I(\mathbf{L^3})](ClO_4)$ (**3**) also affords two crystallographically independent Cu^I-complex ions in the crystal (see Table 3). Notably, the phenyl ring of the ligand sidearm of $\mathbf{L^3}$ comes closer to the cuprous ion, making a coordinative interaction in a η^2 fashion (Figure 2). Thus, the cuprous ion in **3** also adapts a distorted tetrahedral geometry, consisting of the three nitrogen atoms of the ligand and the C(19)−C(20) moiety of the phenyl ring (C(42)−C(43) in molecule 2). This bonding interaction is unsymmetrical, Cu(1)−C(19), 2.251(4) Å; Cu(1)−C(20), 2.375(5) Å in molecule 1 and Cu(2)−C(42), 2.242(4) Å; Cu(2)−C(43), 2.189(4) Å in molecule 2, and these values are comparable to the Cu−C distances in the known $Cu^I-\eta^2$-benzene complexes (2.09−2.30 Å)[15,16] and in the recently reported $Cu^I-\eta^2$-naphthalene **6** (2.129, 2.414 Å)[17] and $Cu^I-\eta^2$-indole **7** (2.228, 2.270 Å)[18] complexes (Scheme 4). Such an interaction between the cuprous ion and the aromatic group of the ligand sidearm is not seen in complex **2** in which CH_3CN molecule occupies the fourth coordination site (Figure 1). In the case of complex **6** as well, coordination of CH_3CN to the metal center prevents the copper(I) complex from making such a Cu^I−aromatic interaction,[17] and the Cu^I−aromatic interaction is easily broken when complex **7** is dissolved in CH_3CN.[18] Thus, the coordinative interaction between the cuprous ion and the aromatics is essentially weak.

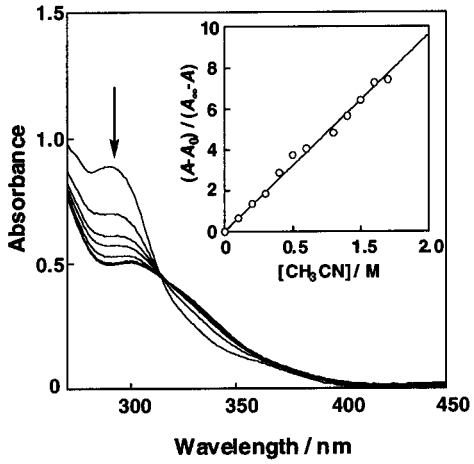

Figure 3. Spectral change for the titration of **1** (1.0×10^{-4} M) with CH_3CN in CH_2Cl_2 at −20 °C. Inset: Plot of $(A - A_0)/(A_\infty - A)$ versus $[CH_3CN]$ based on the absorption change at $A = 290$ nm.

Scheme 5

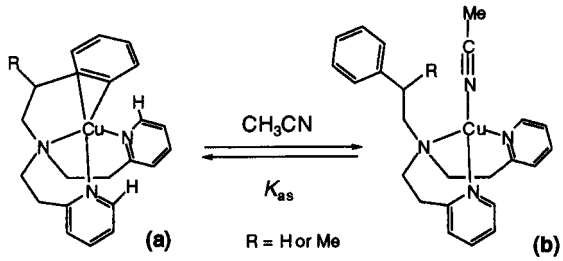

Physicochemical Properties and Reactivity in Solution. UV−visible spectra of $[Cu^I(\mathbf{L^1})](ClO_4)$ (**1**),[5a] $[Cu^I(\mathbf{L^2})(CH_3CN)](ClO_4)$ (**2**·CH_3CN), and $[Cu^I(\mathbf{L^3})](ClO_4)$ (**3**) in CH_2Cl_2 are presented in Figure S1.[19] The complex **3** exhibits an absorption band at 290 nm ($\epsilon = 9700\ M^{-1}\ cm^{-1}$) that can be assigned to the metal−to−phenyl charge transfer (MLCT), as suggested for complex **7** (metal−to−indole) by Shimazaki et al (308 nm, $\epsilon = 18000\ M^{-1}\ cm^{-1}$).[18,20] A similar absorption band at 290 nm is also observed with complex **1** (Figure S1). This suggests that there is a similar Cu^I−phenyl interaction within **1** when it is dissolved in a nonpolar solvent, such as CH_2Cl_2. On the other hand, however, complex **2**·CH_3CN does not show such an absorption band around 300 nm in CH_2Cl_2 (Figure S1), indicating that the coordination of CH_3CN in **2**·CH_3CN is rather strong so as to prevent the Cu^I−phenyl interaction as discussed above.

To confirm this idea, titration of **1** by CH_3CN was carried out in CH_2Cl_2 at −20 °C (Scheme 5). Figure 3 shows a spectral change of the titration. The absorption band at 290 nm due to the Cu^I−phenyl interaction decreases while increasing the added CH_3CN concentration, and the final spectrum of the titration resembles the spectrum of **2**·CH_3CN in CH_3CN. The association

(14) Nagao, H.; Komeda, N.; Mukaida, M.; Suzuki, M.; Tanaka, K. *Inorg. Chem.* **1996**, *35*, 6809−6815.
(15) Turner, R. W.; Amma, E. L. *J. Am. Chem. Soc.* **1966**, *88*, 1877−1882.
(16) Dines, M. B.; Bird, P. H. *J. Chem. Soc., Chem. Commun.* **1973**, 12.
(17) Striejewske, W. S.; Conry, R. R. *Chem. Commun.* **1998**, 555−556.
(18) Shimazaki, Y.; Yokoyama, H.; Yamauchi, O. *Angew. Chem., Int. Ed.* **1999**, *38*, 2401−2403.

(19) See Supporting Information.
(20) The Cu^I−phenyl interaction in the cuprous complex is now being investigated in more detail using a series of *p*-substituted phenyl derivatives of ligand $\mathbf{L^1}$.[5a]

constant K_{as} = [**1**·CH_3CN]/[**1**][CH_3CN] at −20 °C has been determined as 6.4 M^{-1} by analyzing the absorption change, as indicated in the inset of Figure 3. The conformational change induced by the CH_3CN coordination has also been indicated by ^1H NMR. Namely, sharp ^1H NMR peaks due to the ethylene linker of **1** (−CH_2−CH_2−Ph) appear at δ = 2.82 and 3.18 (both triplet, J = 6.1 Hz) in CD_2Cl_2, while those peaks become a broad singlet (δ = 3.0) in CD_3CN. Thus, the two methylene groups of the ethylene linker are nonequivalent as a result of the coordination of the phenyl group in CD_2Cl_2, while such a Cu^I−phenyl interaction is broken in CD_3CN, letting the two methylene groups be nearly magnetically equivalent. In addition, the 6-proton of the pyridine nucleus (H_{py-6}) at δ = 8.07 in CD_2Cl_2 shifts to δ = 8.46 in CD_3CN. Such a downfield shift of H_{py-6} may be due to the disappearance of a ring current effect by the phenyl group, as shown in Scheme 5, where the phenyl group in conformation (a) sits right above the H_{py-6} to induce the upfield shift of H_{py-6}, whereas such a ring current effect by the phenyl ring disappears in conformation (b). The Cu^I−phenyl interaction in complex **1** is further supported by ^{13}C NMR in CD_2Cl_2. Namely, the ^{13}C NMR peaks of the phenyl ring of **1** appear at 123.1 (C_4), 127.43 ($C_{2,6}$), 129.36 ($C_{3,5}$), and 138.92 (C_1) ppm, which are rather similar to those of **3** (121.20, 127.60, 129.44, and 138.93 ppm in CD_2Cl_2), which has the Cu^I−phenyl interaction, but are relatively different from those of **2** (127.09, 128.55, 129.12, and 140.20 ppm in CD_2Cl_2) in which such an interaction is absent.

The K_{as} value of **3** has also been determined as 0.21 M^{-1} in the same way. The significantly smaller K_{as} value of **3** as compared with that of **1** clearly demonstrates that the Cu^I−phenyl interaction, which is essentially weak in **1**, is enhanced significantly in complex **3**. The methyl group of the ligand sidearm of $\mathbf{L^3}$ may occupy a less crowded space in complex **3** (conformation (a) in Scheme 5), placing the phenyl group on the cuprous ion to stabilize the Cu^I−phenyl interaction entropically.[20]

Complex **2**·CH_3CN exhibited a reversible redox couple at 0.30 V versus Fc/Fc^+ (ferrocene/ferrocenium) in CH_2Cl_2, as shown in Figure S2.[19] The good reversibility of the cyclic voltammetry indicates that the coordination of CH_3CN in **2**·CH_3CN is maintained during the electrochemical redox process. In other words, the coordination of CH_3CN in **2**·CH_3CN is strong enough to keep the four-coordinate copper ion, as discussed above. On the other hand, **1** and **3** provided quasi-reversible redox couples at lower potentials (0.08 and 0.07 V versus Fc/Fc^+, respectively), but the reversibility of their cyclic voltammetry became worse ($\Delta E_{1/2}$ = 0.53 and 0.35 V, respectively) as compared with the case of complex **2**·CH_3CN ($\Delta E_{1/2}$ = 0.17 V). This suggests that a larger conformational change occurs during the electrochemical redox process in the cases of **1** and **3**. In the previous study, we reported the crystal structure of the copper(II) complex of ligand $\mathbf{L^1}$, in which there is no interaction between the cupric ion and the aromatic pendant.[4] Thus, the conformational changes in **1** and **3** could be largely attributed to the change of position of the ligand sidearm, i.e., Cu^I−phenyl interaction in the copper(I) state while little interaction between Cu^{II} and the phenyl group in the copper(II) state. The higher redox potential of **2**·CH_3CN (0.30 V) as compared with those of others (0.08 and 0.07 V) can be attributed to the bound CH_3CN, which stabilizes the copper(I) state of the complex. The 6-methyl group in $\mathbf{L^2}$ may also result in increase of $E_{1/2}$, since Tanaka and co-workers have demonstrated that introduction of the 6-methyl group induces a positive shift in $E_{1/2}$ of the copper(II) complexes of TMPA ligands.[14]

Scheme 6

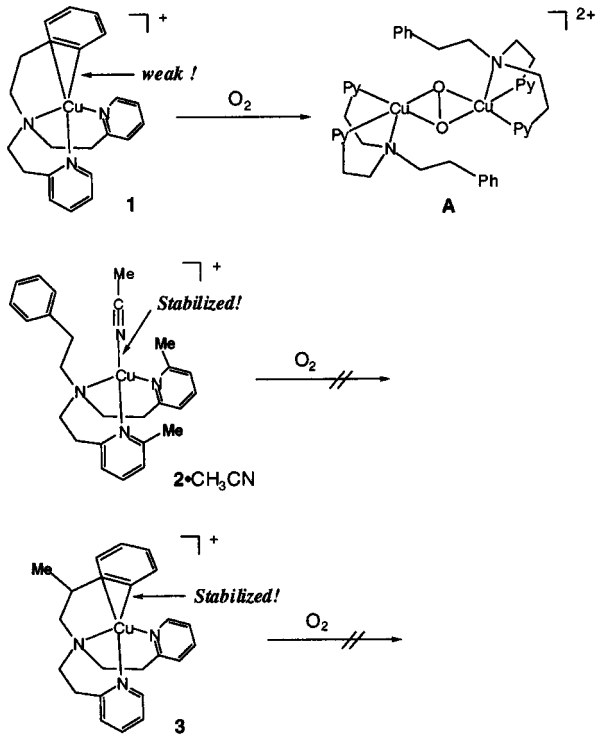

Complex **1** is known to react with O_2 rapidly to generate a peroxo species at low temperature (−80 °C), as illustrated in Scheme 6.[4,5a] In sharp contrast to this, neither **2**·CH_3CN nor **3** reacts with dioxygen at ambient temperature (Scheme 6). The high oxidation potential of **2**·CH_3CN (0.30 V versus Fc/Fc^+) as compared with **1** (0.08 V vs Fc/Fc^+) is certainly an important factor for the stability toward dioxygen. The strong binding of CH_3CN to Cu^I in **2**·CH_3CN may also prohibit the initial coordination of O_2 to the metal center, which is required for formation of the peroxo species from **1** and O_2.[5a] In the case of complex **1**, O_2 can easily bind to the copper ion in place of the weak Cu^I−phenyl bonding, as suggested by the larger K_{as} value. In the case of complex **3**, the stronger Cu^I−phenyl interaction, as demonstrated by the smaller K_{as} value, may be the main factor for prohibiting the direct interaction of the metal ion with dioxygen, since the redox potential of **3** (0.07 V versus Fc/Fc^+) is essentially the same as the value of **1** (0.08 V versus Fc/Fc^+).

In conclusion, the small perturbation induced by the methyl substitution at the 6-position of the pyridine nucleus in $\mathbf{L^2}$ and at the benzylic position of the ligand sidearm in $\mathbf{L^3}$ leads to a drastic change in the structure and reactivity of the copper(I) complexes. Because of a repulsive interaction between the 6-methyl group of $\mathbf{L^2}$ and the metal ion, the cuprous complex resists having a three-coordinate geometry with a shorter Cu−N bond length, such as found in complex **5** (∼1.88 Å). Thus, the copper(I) complex of $\mathbf{L^2}$ tends to have a four-coordinate tetrahedral geometry with a longer Cu−N distance (1.98∼2.13 Å) in which CH_3CN occupies the fourth coordination site. Such a steric effect by the 6-methyl group of $\mathbf{L^2}$ makes the binding of CH_3CN to the metal ion rather strong. Thus, the reactivity of **2**·CH_3CN toward O_2 is almost lost. On the other hand, the methyl group at the benzylic position of $\mathbf{L^3}$ reduces the degree of freedom of the sidearm movement to enhance the stability of the Cu^I−phenyl interaction. In this case as well, a direct interaction between the cuprous ion and O_2 is prohibited due to the stable Cu^I−phenyl interaction. These results will provide

important insights into modulation of the structure and reactivity of copper(I) complexes.

Experimental Section

General. All chemicals used in this study except the ligands and the complexes were commercial products of the highest available purity and were further purified by the standard methods, if necessary.[21] 6-Methyl-2-vinylpyridine was kindly supplied by Koei Chemical Co. Ltd, and was purified by fractional distillation. Synthetic procedures of ligand $\mathbf{L^1}$ and its copper(I) complex were reported previously.[5a] FT−IR spectra were recorded with a Shimadzu FTIR-8200PC. UV−vis spectra were measured using a Hewlett-Packard HP8453 diode array spectrophotometer with a Unisoku thermostated cell holder designed for low-temperature measurements. Mass spectra were recorded with a JEOL JMS-700T Tandem MS station. ^{1}H NMR spectra were recorded on a JEOL FT−NMR Lambda 300WB or a Bruker Advance 600.

The cyclic voltammetry (CV) measurements were performed on an ALS-630A electrochemical analyzer in anhydrous CH_2Cl_2 containing 0.1 M NBu_4ClO_4 as supporting electrolyte. The Pt working electrodes were polished with a polishing alumina suspension and rinsed with CH_2Cl_2 before use. The counter electrode was a Pt wire. A silver pseudo reference electrode was used, and the potentials were determined using the ferrocene/ferricenium (Fc/Fc^+) couple as a reference. All electrochemical measurements were carried out at 25 °C under an atmospheric pressure of Ar in a glovebox (Miwa Co. Ltd.).

Synthesis of Ligands. Ligands $\mathbf{L^2}$ and $\mathbf{L^3}$ were prepared by a Michael addition of phenethylamine to 6-methyl-2-vinylpyridine and of β-methylphenethylamine to 2-vinylpyridine, respectively, in refluxing methanol containing acetic acid, and the products were purified by flash column chromatography (SiO_2) as reported previously.[5a] The structure of the products were confirmed by ^{1}H NMR.

***N,N*-Bis[2-(6-methylpyridin-2-yl)ethyl]phenylethylamine ($\mathbf{L^2}$).** Pale brown oil; ^{1}H NMR (300 MHz, $CDCl_3$): δ 2.52 (6 H, s, $-CH_3$), 2.67−2.83 (4 H, m, $-CH_2-CH_2$-), 2.85−3.00 (8 H, m, $-CH_2-CH_2$-), 6.83 (2 H, d, J = 7.5 Hz, H_{py-3} or H_{py-5}), 6.95 (2 H, d, J = 7.5 Hz, H_{py-3} or H_{py-5}), 7.10−7.27 (5 H, m, C_6H_5), 7.42 (2 H, t, J = 7.5 Hz, H_{py-4}).

***N,N*-Bis[2-(2-pyridyl)ethyl]-β-methylphenylethylamine ($\mathbf{L^3}$).** Pale brown oil; ^{1}H NMR (300 MHz, $CDCl_3$): δ 1.12 (3 H, d, J = 6.6 Hz, $-CH_3$), 2.53−2.97 (11 H, m, −CH- and $-CH_2-CH_2$-), 7.05−7.28 (7 H, m, aromatic H), 7.49 (2 H, dt, J = 1.7 and 7.7 Hz, H_{py-4}), 8.52 (2 H, d, J = 4.3 Hz, H_{py-6}).

Synthesis of Copper(I) Complexes. $[Cu^I(\mathbf{L^2})\cdot CH_3CN]ClO_4$ ($\mathbf{2}\cdot CH_3CN$). Ligand $\mathbf{L^2}$ (126.1 mg, 0.35 mmol) was treated with $[Cu^I(CH_3CN)_4]ClO_4$ (112.3 mg, 0.35 mmol) in CH_2Cl_2 (5 mL) under Ar atmosphere. After stirring for 30 min at room temperature, the insoluble material was removed by filtration. Addition of ether (100 mL) to the filtrate gave a pale yellow powder that was precipitated by allowing the mixture to stand for several minutes. The supernatant was then removed by decantation, and the remaining pale yellow solid was dissolved in CH_3CN (5 mL). Addition of ether (100 mL) to the filtrate gave a pale yellow powder that was precipitated by allowing the mixture to stand for several minutes. The supernatant was then removed by decantation, and the remaining pale yellow solid was washed with ether three times and dried (41% yield). All procedures were done in a glovebox ($[O_2]$ < 0.1 ppm). ^{1}H NMR (600 MHz, acetone-d_6): δ 2.04 (3 H, s, bound CH_3CN), 2.73−2.80 (4 H, m, $-CH_2-CH_2-Ph$), 2.90 (6 H, s, $-CH_3$), 3.20 (4H, br, $-CH_2-CH_2-Py$ or $-CH_2-CH_2-Py$), 3.31 (4 H, t, $-CH_2-CH_2-Py$ or $-CH_2-CH_2-Py$), 7.06−7.21 (5 H, m, aromatic H), 7.47 (2 H, t, J = 7.7 Hz, H_{py-3} or H_{py-5}), 7.54 (2 H, d, J = 7.7 Hz, H_{py-3} or H_{py-5}), 7.97 (2 H, t, J = 7.7 Hz, H_{py-4}). FT-IR (KBr): 1105, 1086, and 625 cm^{-1} (ClO_4^-). FAB−MS (pos), m/z 422.28 (M^+). Anal. for $[Cu^I(\mathbf{L^2})\cdot CH_3CN]ClO_4$. Calcd for $C_{26}H_{32}O_4N_4CuCl$: C, 55.41; H, 5.72; N, 9.94. Found: C, 55.28; H, 5.66; N, 9.67.

$[Cu^I(\mathbf{L^3})]ClO_4$ (3). This compound was prepared in a manner similar to that described above using ligand $\mathbf{L^3}$ (172.7 mg, 0.5 mmol) and $[Cu^I(CH_3CN)_4]ClO_4$ (160.1 mg, 0.5 mmol); 52% yield. All procedures were done in a glovebox ($[O_2]$ < 0.1 ppm). ^{1}H NMR (300 MHz, acetone-d_6): δ 1.20 (3 H, d, J = 6.6 Hz, $-CH_3$), 2.65−3.71 (11 H, m, −CH- and $-CH_2-CH_2$-), 7.29−7.47 (9 H, m, aromatic H, H_{py-3}, and H_{py-5}), 7.49 (2 H, br, H_{py-4}), 8.16−8.32 (2 H, br, H_{py-6}). FT-IR (KBr): 1121, 1089, and 625 cm^{-1} (ClO_4^-). FAB−MS (pos.), m/z 408.28 (M^+). Anal. for $[Cu^I(\mathbf{L^3})]ClO_4$. Calcd for $C_{23}H_{27}O_4N_3CuCl$: C, 54.33; H, 5.35; N, 8.26. Found: C, 54.24; H, 5.30; N, 8.27.

Caution! The perchlorate salts used in this study are all potentially explosive and should be handled with care.

X-ray Structure Determination. Single crystals of $\mathbf{2}\cdot CH_3CN$ and **3** suitable for X-ray structural analysis were obtained by vapor diffusion of ether into a CH_2Cl_2 solution of the complex. In the case of $\mathbf{2}\cdot CH_3CN$, a few drops of CH_3CN was added to the CH_2Cl_2 solution of $\mathbf{2}\cdot CH_3CN$. The single crystal was mounted on a glass fiber. Data of X-ray diffraction were collected by a Rigaku RAXIS−RAPID imaging plate two-dimensional area detector using graphite-monochromated Mo Kα radiation (λ = 0.71070 Å) to 2θ max of 55.0°. All the crystallographic calculations were performed by using the Crystal Structure software package of the Rigaku Corporation and Molecular Structure Corporation (version 1.01, 2000). The crystal structure was solved by direct methods and refined by full-matrix least squares using SIR-92. All non-hydrogen and hydrogen atoms were refined anisotropically and isotropically, respectively. Summary of the fundamental crystal data and experimental parameters for structure determinations is given in Table 1. The experimental details including data collection, data reduction, structure solution and refinement, the atomic coordinates, and B_{iso}/B_{eq}; anisotropic displacement parameters and intramolecular bond distances and angles have been deposited in the Supporting Information.

Acknowledgment. This work was partially supported by Grants-in-Aid for Scientific Research on Priority Area (Nos. 11228205, 11228206) and Grants-in-Aid for Scientific Research (No. 13480189) from the Ministry of Education, Science, Culture, and Sports, Japan. The authors also acknowledge Ms. Masumi Doe of Osaka City University for her help in obtaining measurements on the 600 MHz NMR.

Supporting Information Available: UV−vis spectra of the cuprous complexes in CH_2Cl_2 (Figure S1), cyclic voltammogram of $\mathbf{2}\cdot CH_3CN$ in CH_2Cl_2 (Figure S2), and X-ray crystallographic files for $\mathbf{2}\cdot CH_3CN$ and **3** in CIF format. This material is available free of charge via the Internet at http://pubs.acs.org.

IC010625D

(21) Perrin, D. D.; Armarego, W. L. F.; Perrin, D. R. *Purification of Laboratory Chemicals*, 4th Edition; Pergamon Press: Elmsford, NY, 1996.